Cell

Polycystin-1 and -2 Dosage Regulates Pressure Sensing

Reza Sharif-Naeini,[1,7] Joost H.A. Folgering,[1,7] Delphine Bichet,[1] Fabrice Duprat,[1] Inger Lauritzen,[1] Malika Arhatte,[1] Martine Jodar,[1] Alexandra Dedman,[1] Franck C. Chatelain,[1] Uwe Schulte,[2] Kevin Retailleau,[3] Laurent Loufrani,[3] Amanda Patel,[1] Frederick Sachs,[4] Patrick Delmas,[5] Dorien J.M. Peters,[6] and Eric Honoré[1,*]

[1]Institut de Pharmacologie Moléculaire et Cellulaire, UMR CNRS 6097, Université de Nice Sophia Antipolis, 06560 Valbonne, France
[2]Logopharm, Schlossstrasse 14, 79232 March, Germany
[3]Institut National de la Santé et de la Recherche Médicale 771, UMR CNRS 6214, Faculté de Médecine, 49045 Angers, France
[4]Single Molecule Biophysics, 301 Cary Hall, State University of New York, Buffalo, NY 14214, USA
[5]Centre de Recherche en Neurophysiologie et Neurobiologie de Marseille, UMR CNRS 6231, Faculté de Médecine, Université de la Méditerranée, CS80011, Boulevard Pierre Dramard, 13344 Marseille Cedex 15, France
[6]Department of Human Genetics, Leiden University Medical Center, P.O. Box 9600, 2300 RC Leiden, Netherlands
[7]These authors contributed equally to this work
*Correspondence: honore@ipmc.cnrs.fr
DOI 10.1016/j.cell.2009.08.045

SUMMARY

Autosomal-dominant polycystic kidney disease, the most frequent monogenic cause of kidney failure, is induced by mutations in the *PKD1* or *PKD2* genes, encoding polycystins TRPP1 and TRPP2, respectively. Polycystins are proposed to form a flow-sensitive ion channel complex in the primary cilium of both epithelial and endothelial cells. However, how polycystins contribute to cellular mechanosensitivity remains obscure. Here, we show that TRPP2 inhibits stretch-activated ion channels (SACs). This specific effect is reversed by coexpression with TRPP1, indicating that the TRPP1/TRPP2 ratio regulates pressure sensing. Moreover, deletion of TRPP1 in smooth muscle cells reduces SAC activity and the arterial myogenic tone. Inversely, depletion of TRPP2 in TRPP1-deficient arteries rescues both SAC opening and the myogenic response. Finally, we show that TRPP2 interacts with filamin A and demonstrate that this actin crosslinking protein is critical for SAC regulation. This work uncovers a role for polycystins in regulating pressure sensing.

INTRODUCTION

Autosomal-dominant polycystic kidney disease (ADPKD) is a multisystem disorder characterized by renal and extrarenal cysts, as well as cardiovascular abnormalities (Arnaout, 2001; Delmas, 2004; Harris and Torres, 2009). Mutations in either *PKD1* or *PKD2* gene, encoding polycystin-1 (TRPP1) or -2 (TRPP2), respectively (for recent nomenclature see Nilius et al., 2007), account for this common hereditary disease (Harris and Torres, 2009). TRPP1 is a large integral membrane glycoprotein with 11 transmembrane domains and an extensive amino-terminal extracellular domain involved in cell-cell, cell-matrix interaction and signaling pathways (for review see Wilson, 2004). TRPP1 interacts with TRPP2, a six transmembrane domain protein of the TRP ion channel family (for review see Giamarchi et al., 2006). Polycystins also interact with multiple partners, including the TRP channel subunits TRPC1 and TRPV4 (Kottgen et al., 2008; Tsiokas et al., 1999), as well as several elements of the cytoskeleton (for reviews see Chen et al., 2008; Delmas, 2004; Harris and Torres, 2009; Wilson, 2004).

By associating through the coiled-coil motifs in their cytosolic carboxy-terminal domains, TRPP1 and TRPP2 have been proposed to form a "receptor-ion channel complex" (Hanaoka et al., 2000). TRPP1 and TRPP2 colocalize at the membrane of the primary cilia of renal epithelial cells and endothelial cells where they are proposed to transduce luminal shear stress (i.e., fluid flow parallel to the cell surface) into a calcium signal (Nauli et al., 2003, 2008). With its large extracellular amino-terminal domain, TRPP1 has been suggested to be a mechanical sensor regulating the opening of the associated calcium-permeable channel TRPP2 (Nauli et al., 2003). Loss of this mechanosensory function (i.e., flow sensing) is thought to result in altered cellular signaling subsequently leading to cyst formation (Nauli and Zhou, 2004).

In endothelial primary cilia, as reported in kidney epithelial cells (Nauli et al., 2003), TRPP1 and TRPP2 are also involved in fluid shear sensing and regulate calcium signaling and nitric oxide release, thus contributing to vasodilation in response to an increase in blood flow (Aboualaiwi et al., 2009; Nauli et al., 2008). However, polycystins are also abundantly expressed in arterial myocytes (Boulter et al., 2001; Qian et al., 2003), which respond to intraluminal pressure that causes wall stretch, instead of flow. An increase in intraluminal pressure causes a gradual depolarization of the vascular smooth muscle cells (VSMCs) that is linked to the opening of nonselective stretch-activated cation channels (SACs), followed by the opening of voltage-gated calcium channels, resulting in an increase in intracellular Ca^{2+} and myocyte constriction (the myogenic or Bayliss response) (Brayden et al., 2008; Hill et al., 2006; Voets and Nilius, 2009). The possible involvement of polycystins in pressure sensing has not yet been investigated.

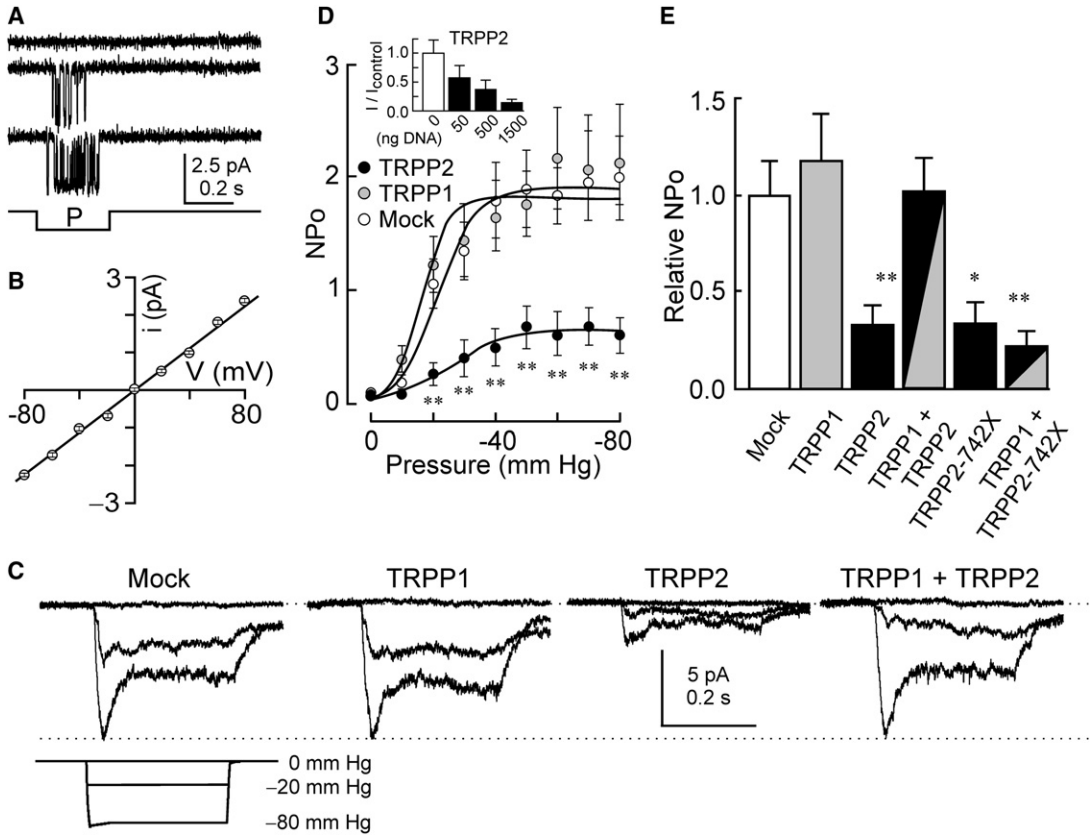

Figure 1. SAC Inhibition by TRPP2

(A) Single-channel currents recorded in the cell-attached patch configuration and induced by increasing negative pipette pressure (0, −10, and −30 mm Hg) in a mock-transfected COS-7 cell at a holding potential of −80 mV. SAC activity was significantly inhibited (−67%, n = 18) by the cup-former cationic amphipath chlorpromazine (50 μM; not shown).

(B) Mean (± standard error of the mean [SEM]) i-V relationship of single SACs from mock-transfected COS-7 cells stimulated with a negative (−30 mm Hg) pressure pulse in the inside out configuration (n = 6).

(C) Mean SAC currents in COS-7 cells transfected with mock, hTRPP1, hTRPP2, and hTRPP1 + hTRPP2 plasmids at a holding potential of −80 mV in the cell-attached patch configuration.

(D) Mean (±SEM) NPo as a function of pressure in cells transfected with the control, hTRPP1, and hTRPP2. Data are fitted with Boltzmann functions ($P_{0.5}$ = −21.7 ± 2.4; −16.1 ± 2.0; and −24.6 ± 5.6 mm Hg; k = 6.1 ± 0.8; 4.3 ± 0.6; and 8.2 ± 1.8; for control, hTRPP1 and hTRPP2 transfected cells, respectively). (Inset) Dose-dependent SAC inhibition by *TRPP2* (n = 31, 10, 20, and 30).

(E) Relative mean (±SEM) NPo at −60 mm Hg for control, hTRPP1, hTRPP2 (or hTRPP2-742X), and hTRPP1 and hTRPP2 (or hTRPP2-742X) cotransfected. n = 40, 40, 30, 40, 20, and 22, for control, hTRPP1, hTRPP2, hTRPP1+hTRPP2, hTRPP2-742X, and hTRPP1+hTRPP2-742X, respectively.

Here, we demonstrate that the TRPP1/TRPP2 ratio regulates SAC activity via the filamin A (FLNa)/F-actin cytoskeletal network and modulates the arterial myogenic response to intraluminal pressure.

RESULTS

TRPP2 Expression Reduces SAC Activity

To determine the effect of TRPP1 and TRPP2 on SAC activity, we expressed the proteins either individually or together in COS cells, an expression system previously used to study mechanosensitive ion channels (Gottlieb et al., 2007; Honoré et al., 2006). In cell-attached recordings of mock-transfected cells, brief negative pressure pulses applied through the recording electrode evoked a gradual and reversible opening of endogenous cation nonselective SACs (Figure 1A), with a single-channel conductance of 29.2 ± 0.3 pS and a reversal potential (E_{rev}) of 0.1 ± 0.3 mV (n = 13; Figure 1B). Surprisingly, while overexpression of TRPP1 alone had no significant effect (Figure 1C), overexpression of TRPP2 produced a dramatic and dose-dependent inhibition of SAC activity (Figures 1C and 1D, inset, and Figure 1E). Neither single-channel conductance, ionic selectivity (see Figure S1 available online), or open probability in patches with a single channel were changed by TRPP2 overexpression. The percentage of active patches was reduced from 94% ± 1% (n = 264) in mock-transfected cells to 70% ± 5% in cells expressing TRPP2 (p < 0.001, n = 90; data not shown). Interestingly, SAC inhibition was also observed with a disease-causing TRPP2 mutant in which a nonsense mutation generates a truncated form of TRPP2 (hTRPP2-742X or the mouse equivalent

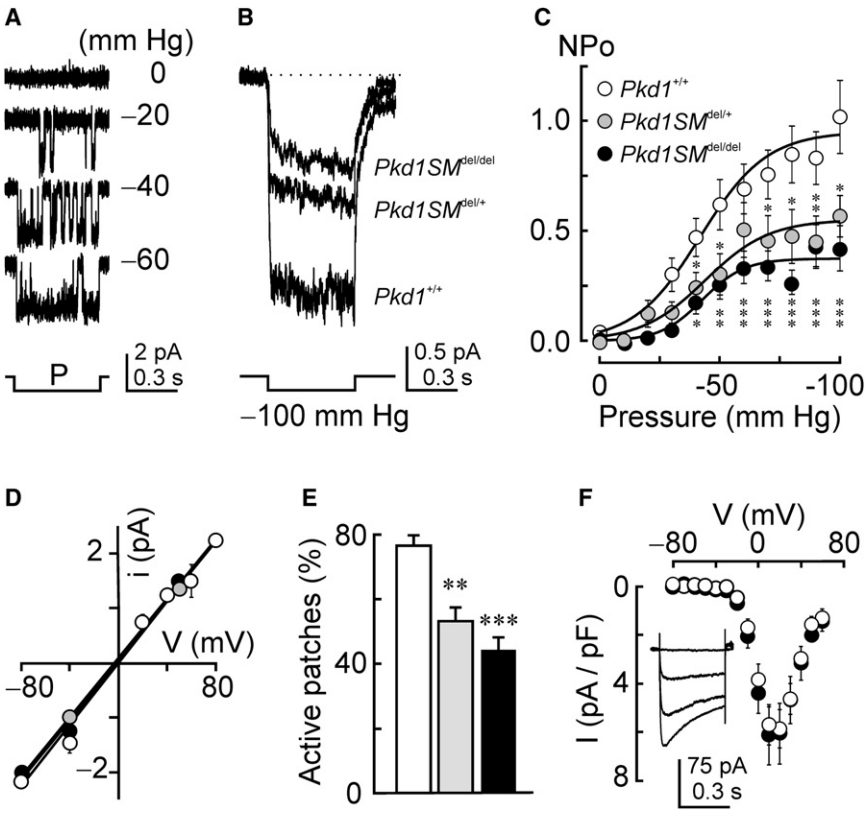

Figure 2. *Pkd1* Inactivation Reduces SAC Activity in Vascular Smooth Muscle Cells

(A) Single-channel currents (cell-attached patch configuration) induced by negative pipette pressures in a $Pkd1^{+/+}$ VSMC at a holding potential of −80 mV.

(B) Mean currents in isolated VSMCs from $Pkd1^{+/+}$, $Pkd1SM^{del/+}$, or $Pkd1SM^{del/del}$ mice. Sample numbers for (B), (C), and (E) are: n = 70, 46, and 64 for $Pkd1^{+/+}$, $Pkd1SM^{del/+}$, and $Pkd1SM^{del/del}$ cells, respectively.

(C) Mean (±SEM) pressure-dependent SAC activity (NPo). Data are fitted with Boltzmann functions ($P_{0.5}$ = −41.8 ± 2.9; −43.9 ± 4.9; and −42.7 ± 3.5 mm Hg; k = 13.8 ± 2.3; 13.3 ± 4.0; 8.8 ± 2.9; for $Pkd1^{+/+}$, $Pkd1SM^{del/+}$, and $Pkd1SM^{del/del}$ cells, respectively).

(D) Mean (±SEM) i-V relationships of single SACs from $Pkd1^{+/+}$ (white circles; n = 11), $Pkd1SM^{del/+}$ (gray circles; n = 18), and $Pkd1SM^{del/del}$ (black circles; n = 8) VSMCs at −50 mm Hg.

(E) Mean percentage (±SEM) of active patches at −100 mm Hg for $Pkd1^{+/+}$ (white bars), $Pkd1SM^{del/+}$ (gray bars), and $Pkd1SM^{del/del}$ (black bars) cells.

(F) Mean (±SEM) nifedipine (2 μM)-sensitive barium currents recorded in the whole-cell configuration in $Pkd1^{+/+}$ (n = 17) and $Pkd1SM^{del/del}$ (n = 15) VSMCs. (Inset) Nifedipine-sensitive barium currents in a $Pkd1^{+/+}$ VSMC stimulated from −60 mV to −50, −10, and 10 mV.

mTRPP2-740X) lacking the ER retention signal (Figures 1E, S2A, and S6) (Mochizuki et al., 1996). This inhibitory effect of TRPP2 on SACs was also present in cell lines originating from different tissues including renal epithelium (LLC-PK1), dorsal root ganglion neurons (F11), and vascular smooth muscle (MOVAS, A7R5, and mouse aortic explants), thus probably representing a fundamental cellular property (Figure S2A). The effect of TRPP2 expression was selective for SACs, as the activity of other channel types, including ASIC and Kv, were not modified by TRPP2 overexpression (Figures S2B and S2C). Moreover, other TRP channels shown to directly interact with TRPP2 and/or claimed to be implicated in mechanotransduction (Christensen and Corey, 2007; Gottlieb et al., 2007; Kottgen et al., 2008; Maroto et al., 2005; Pedersen and Nilius, 2007; Spassova et al., 2006; Tsiokas et al., 1999), including TRPC1, TRPV4 and TRPC6, failed to affect SAC activity (Figure S2D).

TRPP1 Reverses SAC Inhibition by TRPP2

Interestingly, coexpression of TRPP1 with TRPP2 reversed the inhibitory effect of TRPP2 on SACs (Figures 1C and 1E). To examine whether the reversal by TRPP1 requires an interaction with TRPP2, we expressed TRPP1 with TRPP2-742X, which lacks the coiled-coil TRPP1 binding domain. TRPP1 could not rescue SAC activity in TRPP2-742X-transfected COS cells (Figure 1E), demonstrating that the reversal of SAC inhibition is dependent on an interaction between TRPP1 and TRPP2. Moreover, this reversal was specific to TRPP1, as coexpression with either TRPC1 or TRPV4, also known to interact with TRPP2 (Kottgen et al., 2008; Tsiokas et al., 1999), failed to reverse SAC inhibition by TRPP2 (Figure S2D). These observations indicate that the dosage of TRPP2 relative to TRPP1 modulates the activity of SACs in expression systems. Here, we detected no significant exogenous channel current expression at the plasma membrane after transient transfection of TRPP1 and/or TRPP2 (wild-type [WT] or 742X) in both MOVAS (data not shown) and COS cells using either single channel or whole cell patch clamp recording configurations (Figure S7).

Pkd1 Inactivation Reduces SAC Activity in Arterial Myocytes

If the TRPP1/TRPP2 dosage modulates SAC activity in a native system known to express both polycystins, we would expect that lowering the expression of TRPP1 may cause a TRPP2-mediated inhibition of SAC activity. We inactivated the *Pkd1* gene selectively in mouse smooth muscle cells using the Cre/lox strategy (with no alteration in the level of expression of *Pkd2* or other relevant TRP subunits; see Experimental Procedures) (Holtwick et al., 2002) and examined SAC activity in VSMCs acutely dissociated from resistance mesenteric arteries of $Pkd1^{+/+}$, $Pkd1SM^{del/+}$, or $Pkd1SM^{del/del}$ mice. Measurements of arterial pressure revealed no significant difference between the *Pkd1* genotypes (Figure S8). In cell-attached patches, brief negative pressure pulses applied through the recording electrode evoked a gradual and reversible opening of SACs (Figure 2A) with biophysical properties similar to those found in COS cells (single-channel conductance: 28.5 ± 0.4 pS; n = 11).

The variability in kinetics (Figures 1C and 2B) can be explained by different viscoelastic properties between VSMCs and COS cells (Sachs and Morris, 1998). Ionic substitutions (E_{rev}: −3.5 ± 2.1 mV, n = 11, with NaCl; −5.2 ± 3.2 mV, n = 12, with sodium gluconate; −30.5 ± 3.8 mV, n = 4, with choline chloride; Figure 2D and data not shown), as well as pharmacological experiments, indicated that these channels were cationic, nonselective, and inhibited by classical blockers of SACs (−78.0 ± 14.0%, n = 13, with 30 μM Gd^{3+} and −89.0 ± 9.0%, n = 7, with 5 μM GsTMx4). Moreover, pressure-induced inward SAC currents at negative membrane potentials could be recorded when Ca^{2+} (or Ba^{2+}) was the only possible charge carrier, thus indicating Ca^{2+} permeability of the channel (Figure S9). Remarkably, the activity of SACs was significantly lower in VSMCs from *Pkd1SM*$^{del/+}$ and *Pkd1SM*$^{del/del}$ compared to *Pkd1*$^{+/+}$ mice (Figures 2B and 2C). The GsTMx4-sensitive SACs component was significantly smaller in arterial myocytes from *Pkd1SM*$^{del/del}$ mice, as compared to those isolated from *Pkd1*$^{+/+}$ mice (Figure S10). Neither the single-channel conductance (Figure 2D) nor the open channel probability (Po) changed in patches with a single channel, indicating that the number of active SACs is decreased in VSMCs from *Pkd1SM*$^{del/+}$ and *Pkd1SM*$^{del/del}$ mice. Indeed, the percentage of active patches (i.e., with SAC opening) was significantly lower in VSMCs of *Pkd1SM*$^{del/+}$ and *Pkd1SM*$^{del/del}$ mice (Figure 2E). The density of the L-type voltage-dependent calcium current, which plays a key role in arterial excitation-contraction coupling, was not different between mesenteric VSMCs isolated from *Pkd1*$^{+/+}$ and *Pkd1SM*$^{del/del}$ mice (5.61 ± 0.81 pA/pF in *Pkd1*$^{+/+}$ compared to 6.05 ± 1.17 pA/pF in *Pkd1SM*$^{del/del}$; at +10 mV; Figure 2F). These data show that in VSMCs reducing TRPP1 expression causes a specific decrease in SAC activity.

Pkd1 Inactivation Impairs the Arterial Myogenic Response

Stretch-activated channels are known to be involved in the myogenic tone, a key function of resistance arteries in response to an increase in intraluminal pressure (Brayden et al., 2008; Hill et al., 2006; Lee et al., 2007; Mederos y Schnitzler et al., 2008). Indeed, specific pharmacological inhibition of SACs with the spider toxin GsMTx4 (Suchyna et al., 2000) significantly reduced the myogenic tone of resistance mesenteric arteries (Figure S11). Because the activity of SACs was significantly reduced in the absence of TRPP1, we examined whether the myogenic contractility of resistance arteries may also be affected. Mesenteric arteries isolated from *Pkd1*$^{+/+}$ mice produced a robust myogenic contraction when intraluminal pressure was increased (Figures 3A and 3B). However, arteries isolated from *Pkd1SM*$^{del/+}$ and *Pkd1SM*$^{del/del}$ mice showed a profound decrease in myogenic tone (Figures 3A and 3B). Furthermore, the threshold pressure for myogenic contraction was significantly shifted to higher pressure in arteries with decreased *Pkd1* expression (Figure 3B). This indicates that these arteries have to be distended further before triggering mechanosensory feedback (Figures 3A and 3B). Additionally, we observed no change in vascular reactivity to KCl or phenylephrine in mesenteric arteries from 12- to 16-week-old *Pkd1SM*$^{del/del}$ mice (Figure 3C), which confirms findings from a related study using 20-week-old *Pkd1*

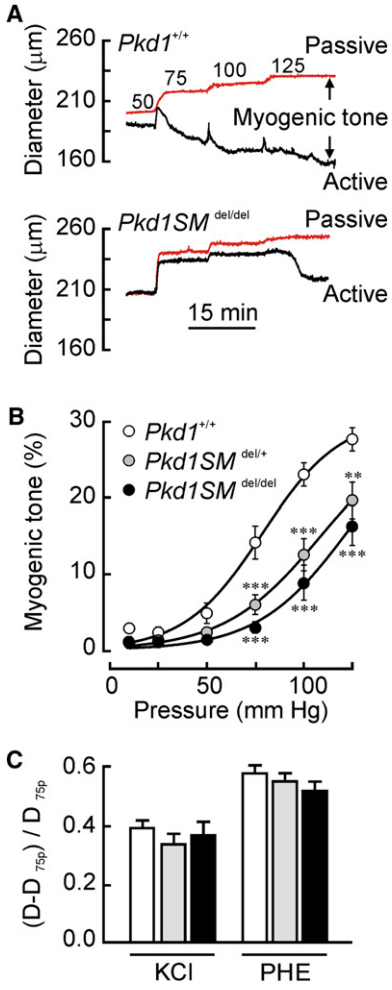

Figure 3. *Pkd1* Inactivation Impairs the Mesenteric Artery Myogenic Response

(A) Changes in lumen diameter in *Pkd1*$^{+/+}$ (top panel) and *Pkd1SM*$^{del/del}$ (lower panel) arteries as a function of pressure. Black traces represent the active curve in the presence of 2.5 mM $CaCl_2$ and red traces represent the passive curve (distensibility) in the absence of $CaCl_2$ and the presence of sodium nitroprusside, papaverine, and EGTA.

(B) Mean (±SEM) myogenic tone (percentage of passive diameter) in *Pkd1*$^{+/+}$ (white symbols), *Pkd1SM*$^{del/+}$ (gray symbols), and *Pkd1SM*$^{del/del}$ (black symbols) arteries. Data are fitted with Boltzmann functions ($P_{0.5}$ = 78.5 ± 3.7; 94.2 ± 8.0; and 101.4 ± 8.5 mm Hg; k = 14.2 ± 2.5; 11.5 ± 2.7; 7.0 ± 1.7; for *Pkd1*$^{+/+}$, *Pkd1SM*$^{del/+}$, and *Pkd1SM*$^{del/del}$ arteries, respectively).

(C) Mean (±SEM) KCl- and phenylephrine-induced contractions in the three genotypes at 75 mm Hg.

(global) heterozygote mice (Morel et al., 2009). These results support the assumption that L-type calcium channel activity was unchanged and that intracellular calcium stores, as well as the contractile apparatus, were not significantly altered by *Pkd1* deletion. Finally, the wall/lumen ratio did not vary between genotypes (Figure S3A). Moreover, the stress-strain curves of mesenteric arteries were identical (Figure S3B), indicating that the contribution of elastin and collagen to arterial wall elasticity was unaltered by *Pkd1* inactivation. Thus, the expression of

TRPP1 in VSMCs appears essential for pressure-dependent mesenteric artery SAC activity and myogenic tone, but does not affect other arterial properties.

Depletion of TRPP2 in TRPP1-Deficient VSMCs Restores Both SAC Activity and Myogenic Tone

We hypothesized that when TRPP2 is released from its interaction with TRPP1, either by lowering TRPP1 expression (*Pkd1SM*$^{del/+}$ *or Pkd1SM*$^{del/del}$) or by overexpressing TRPP2, it impairs SAC activity and lowers myogenic tone. Therefore, reducing the expression of TRPP2 in arteries lacking *Pkd1* should restore SAC opening and consequently the myogenic tone. Indeed, knocking down *Pkd2* by about 80% with an siRNA (Figure S4) increased SAC activity in *Pkd1SM*$^{del/del}$ VSMCs and the percentage of active patches (Figures 4A–4C). Additionally, *Pkd2* knockdown restored myogenic tone in *Pkd1SM*$^{del/del}$ mesenteric arteries (Figures 4D and 4E). These results suggest that free TRPP2 (unbound to TRPP1) is responsible, at least in large part, for the decrease in SAC function and myogenic tone in *Pkd1SM*$^{del/+}$ and *Pkd1SM*$^{del/del}$ arteries.

Role of the Actin Cytoskeleton in SAC Inhibition by TRPP2

The cortical F-actin cytoskeleton exerts a tonic inhibitory control over SAC activity, presumably by reducing the amount of stretch-induced increase in bilayer tension sensed by the channel protein (Lauritzen et al., 2005; Morris, 2001). Because TRPP2 is known to interact with various cytoskeletal elements (for reviews see Chen et al., 2008; Delmas, 2004; Harris and Torres, 2009; Wilson, 2004), we examined whether SAC inhibition by the F-actin cytoskeleton may be enhanced in the presence of TRPP2. Using the actin monomer-sequestering agent latrunculin A, we demonstrate that disruption of the F-actin cytoskeleton increased SAC activity in COS cells (Figures 5A and 5B), thus confirming the tonic inhibitory influence of the actin cytoskeleton. A similar effect on SAC activity was observed when we used the barbed-end capping agent cytochalasin D at concentrations known to induce F-actin depolymerization through capping-induced growth arrest and actin dimer formation (Figure 5B). Remarkably, these treatments fully reversed SAC inhibition by TRPP2 in COS cells and restored channel activity (Figures 5A and 5B). Latrunculin A similarly increased SAC activity in VSMCs from *Pkd1SM*$^{+/+}$ and *Pkd1SM*$^{del/del}$ arteries and suppressed the difference between both genotypes (Figure 5C). However, microtubule-disrupting agents, including colchicine or nocodazole, did not modify SAC inhibition by TRPP2 (Figure 5B). Conversely, actin stabilization by jasplakinolide inhibited SAC activity and mimicked the effect of TRPP2 in COS cells (Figure 5B). These data demonstrate that the F-actin cytoskeleton is involved in SAC inhibition by TRPP2.

Filamin A Interacts with TRPP2 and Is Required for SAC Inhibition

In a search for proteins that bind to TRPP2, we performed a proteomic screen in the mouse VSMC line MOVAS. Besides known TRPP2 partners, including TRPP1 and the $InsP_3$ receptor, we identified the actin crosslinking protein FLNa (Glogauer et al., 1998; Kainulainen et al., 2002; Stossel et al., 2001) (Table S1).

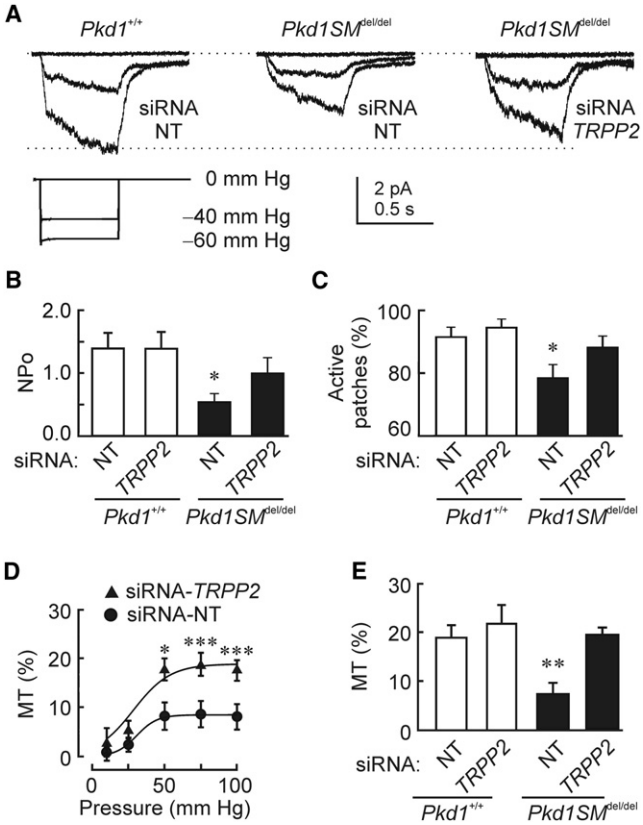

Figure 4. Knocking down TRPP2 Rescues SAC Activity and Myogenic Tone in the *Pkd1* Knockout Mesenteric Arteries

(A) Mean SAC currents in VSMCs treated with siRNA-NT (n = 83 for *Pkd1*$^{+/+}$ and 86 for *Pkd1SM*$^{del/del}$ cells) or siRNA-*TRPP2*-A (n = 47) at a holding potential of −80 mV.

(B) Mean (±SEM) SAC activity (NPo at −60 mm Hg) of VSMC from *Pkd1*$^{+/+}$ (white bars) and *Pkd1SM*$^{del/del}$ (black bars) arteries treated with siRNA-NT (n = 83 for *Pkd1*$^{+/+}$ and 93 for *Pkd1SM*$^{del/del}$ cells) or siRNA-*TRPP2*-A (n = 44 for *Pkd1*$^{+/+}$ and 49 for *Pkd1SM*$^{del/del}$ cells). *p < 0.05, represents significant difference from *Pkd1*$^{+/+}$ siRNA-NT. Similar results were obtained with a second siRNA against *TRPP2* (siRNA-*TRPP2*-B; not shown).

(C) Mean (±SEM) percentage of active patches in *Pkd1*$^{+/+}$ and *Pkd1SM*$^{del/del}$ cells transfected with either NT or *TRPP2*-A siRNAs. Same n values as in (B). Asterisk represents significant difference from *Pkd1*$^{+/+}$ siRNA-NT.

(D) Mean (±SEM) myogenic tone (MT) in *Pkd1SM*$^{del/del}$ arteries treated with the siRNA-NT (n = 9) or the siRNA-*TRPP2*-A (n = 7) as a function of intraluminal pressure.

(E) Mean (±SEM) myogenic tone (MT) at 75 mm Hg in *Pkd1*$^{+/+}$ and *Pkd1SM*$^{del/del}$ arteries treated with siRNA-NT (n = 5 for *Pkd1*$^{+/+}$ and 10 for *Pkd1SM*$^{del/del}$) or siRNA-*TRPP2*-A (n = 4 for *Pkd1*$^{+/+}$ and 9 for *Pkd1SM*$^{del/del}$). **p < 0.01 and ***p < 0.001 represent significant difference from *Pkd1SM*$^{del/del}$ siRNA-*TRPP2*.

Immunoprecipitation in cotransfected cells confirmed this interaction (Figures 6A and S12). To determine whether the effect of TRPP2 on SAC activity is dependent on FLNa, we expressed TRPP2 in a human melanoma cell line (M2 or FLNa KO) that does not express FLNa and in M2 cells stably transfected with FLNa (A7 or FLNa WT) (Cunningham et al., 1992) (Figure S5). The single-channel conductance of SACs was similar in both cell lines (29.1 ± 0.8 pS for FLNa KO cells, n = 37, compared to 29.2 ± 0.8 pS for FLNa WT cells, n = 27; p = 0.888), but the net

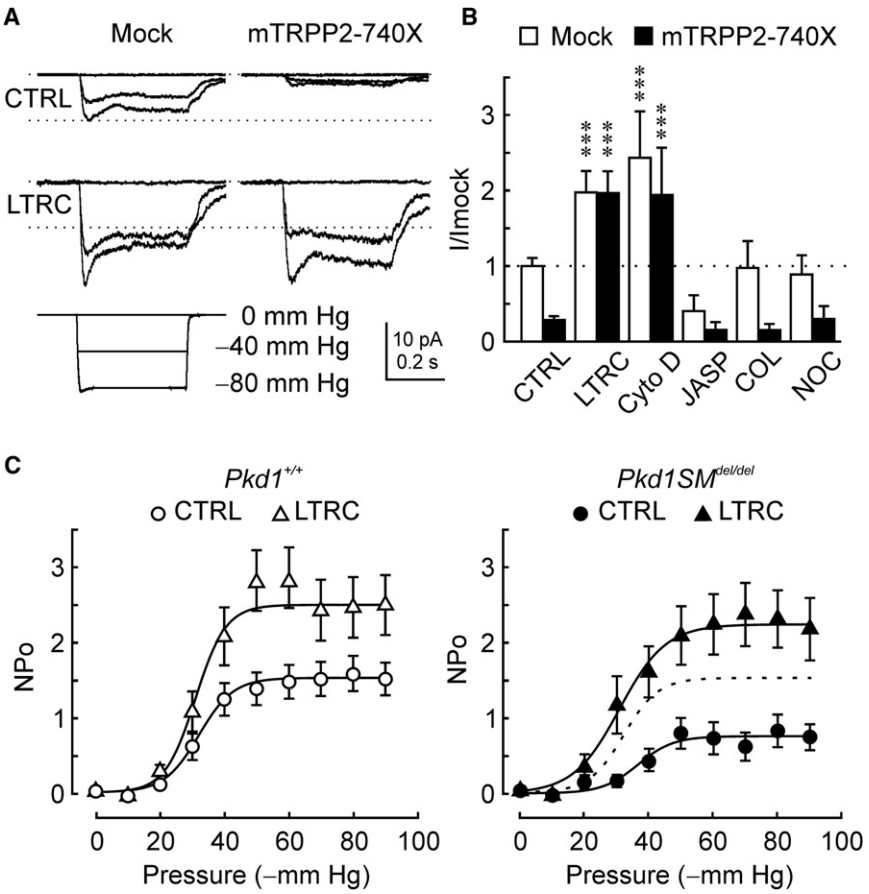

Figure 5. Disruption of the Actin Cytoskeleton Reverses SAC Inhibition by TRPP2

(A) Mean SAC currents (cell attached patch configuration) at a holding potential of −80 mV in COS-7 cells transfected with empty expression vector (mock) or mTRPP2-740X. Cells were incubated with the vehicle 0.1% DMSO (CTRL) (top panels; n = 89 and 80 for control and mTRPP2-740X, respectively) or with 3 μM latrunculin A (bottom panels; n = 38 and 37 for control and mTRPP2-740X, respectively) (LTRC) for 1 hr prior recordings.

(B) Mean (±SEM) SAC currents in COS-7 cells expressing empty expression vector (mock shown in white) or mTRPP2-740X (shown in black). Cells were incubated with 0.1% DMSO (n = 89 and 80 for mock and mTRPP2-740X, respectively), 3 μM latrunculin A (LTRC) for 1 hr (n = 38 and 37 for mock and mTRPP2-740X, respectively), 1 μM cytochalasin D (cyto D) for 1 hr (n = 10 for both mock and mTRPP2-740X), 3 μM jasplakinolide (JASP) for 1 hr (n = 10 for both mock and mTRPP2-740X), 500 μM colchicine (COL) for 2 hr (n = 10 for both mock and mTRPP2-740X), or 10 μM nocodazole (NOC) for 1.5 hr (n = 10 for both mock and mTRPP2-740X). All values are given as relative to the maximum control current in the mock transfected cells (−80 mm Hg) in the cell-attached configuration at a holding potential of −80 mV. The difference between mock and mTRPP2-740X is only significant ($p < 0.05$) in the CTRL, COL, and NOC-treated conditions.

(C) Mean (±SEM) pressure-dependent SAC activity (NPo) of *Pkd1*$^{+/+}$ (left panel) and *Pkd1SM*$^{del/del}$ (right panel) cells recorded in the cell attached configuration at a holding potential of −80 mV. Cells were incubated with 0.1% DMSO (open and closed circles; n = 83 and 45 for *Pkd1*$^{+/+}$ and *Pkd1SM*$^{del/del}$, respectively) or with 3 μM latrunculin A (open and closed triangles; n = 68 and 47 for *Pkd1*$^{+/+}$ and *Pkd1SM*$^{del/del}$, respectively) for 24 hr before recordings. Data are fitted with Boltzmann functions ($P_{0.5}$ = −32.1 ± 0.6; −31.0 ± 1.9; −36.7 ± 2.2; and −31.0 ± 1.2 mm Hg; k = 5.4 ± 0.5; 4.7 ± 1.8; 5.5 ± 1.9; and 7.2 ± 1.0; for *Pkd1*$^{+/+}$ DMSO treated, *Pkd1*$^{+/+}$ latrunculin treated, *Pkd1SM*$^{del/del}$ DMSO treated, and *Pkd1SM*$^{del/del}$ latrunculin treated, respectively). Dotted curve in the right panel shows the Boltzmann function for DMSO-treated *Pkd1*$^{+/+}$ cells. The difference was significant ($p < 0.01$) between *Pkd1*$^{+/+}$ and *Pkd1SM*$^{del/del}$ when DMSO treated, but not after latrunculin A treatment.

channel activity was significantly higher in FLNa KO cells (Figures 6B–6D). Importantly, while the inhibition of SAC activity by TRPP2 was prominent in FLNa WT cells, it was absent in FLNa KO cells (Figure 6D). This indicates that FLNa is critically required for the inhibitory effect of TRPP2 on SACs.

DISCUSSION

Although polycystins have been associated with the mechanosensory function of flow sensing in both epithelial and endothelial cells (Nauli et al., 2003, 2008), how they contribute to cellular mechanosensitivity still remains unknown. In this study, we demonstrate that SAC activity is strongly reduced in VSMC membranes and arterial myogenic tone is impaired when there is an overabundance of free TRPP2, either by decreasing TRPP1 or increasing TRPP2. The inhibitory effect is specific to TRPP2 based on the fact that expression of other TRP channel subunits, including TRPC1 and TRPC6, has no effect on SAC activity. Moreover, the activity of Kv and ASIC was unaffected by TRPP2 overexpression and there was no change in L-type Ca^{2+} channel activity following inactivation of *Pkd1*, indicating that TRPP2 specifically regulates the activity of SACs.

Our results differ from the proposed role of the TRPP1/TRPP2 complex as a flow sensor in the primary cilium of renal epithelial and endothelial cells where inactivation of either TRPP1 or TRPP2 impairs flow sensing (Nauli et al., 2003, 2008). In VSMCs, it is the TRPP1/TRPP2 ratio that regulates the activity of native nonselective cation SACs. In the case of pressure sensing by arterial myocytes, TRPP2 inhibits mechanosensitivity and TRPP1 reverses this inhibition, while in the case of flow sensing by the primary cilium, both TRPP1 and TRPP2 promote mechanosensitivity (Nauli et al., 2003, 2008).

We demonstrated that although TRPP1 and TRPP2 are known to function as a complex (Hanaoka et al., 2000), TRPP2 can independently influence SAC activity, and that TRPP1 reverses this effect. Other independent functions for TRPP2 have been previously reported. For instance, in nodal cells, where TRPP1 is absent, TRPP2 has been implicated in the specification of the left-right axis (Pennekamp et al., 2002). Antagonism between TRPP1 and TRPP2 has also been shown in rat sympathetic

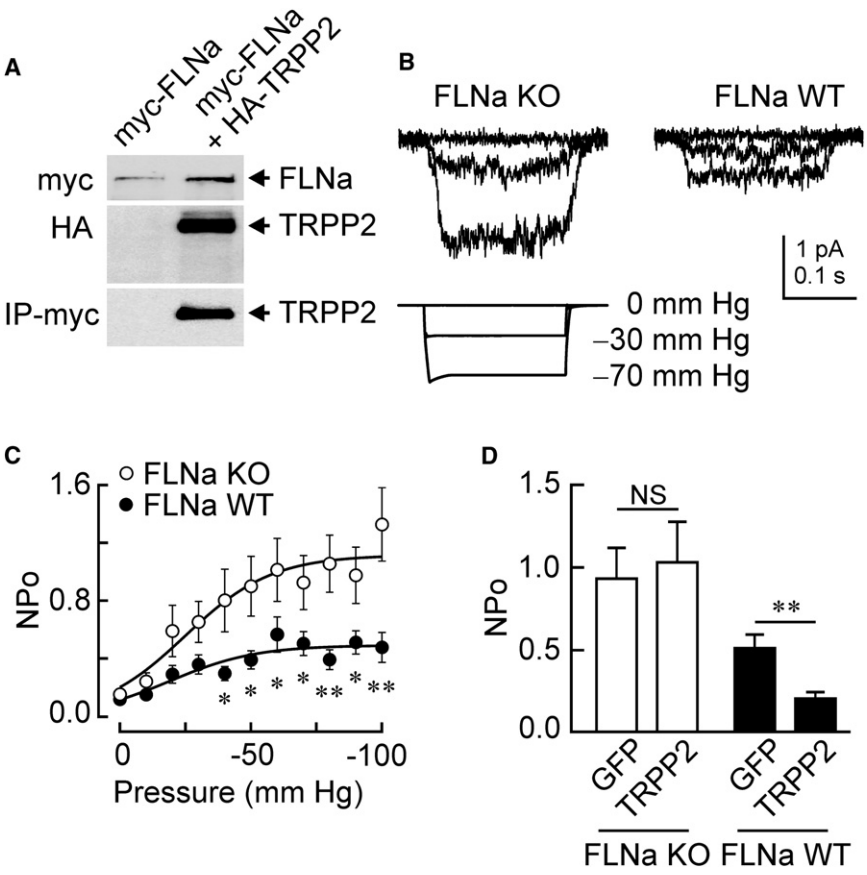

Figure 6. TRPP2 Inhibition of SAC Activity Requires FLNa

(A) Coimmunoprecipitation experiment demonstrating the interaction between HA-tagged TRPP2 and myc-tagged FLNa in cotransfected COS cells. left lane, transfected with myc-tagged FLNa; right lane, transfected with myc-tagged FLNa and HA-tagged TRPP2. See Figure S12 for whole blots.

(B) Mean SAC currents in M2 (FLNa KO) (n = 63) and A7 (n = 66) cells (FLNa WT) at a holding potential of −80 mV.

(C) Mean (±SEM) NPo as a function of pressure in FLNa KO (white) and FLNa WT (black) cells. Expression of TRPP2 in FLNa KO (n = 48) and FLNa WT (n = 57) cells did not affect single SAC conductance (data not shown). Data are fitted with Boltzmann functions ($P_{0.5}$ = −25.0 ± 4.5 mmHg; −19.2 ± 5.6 mmHg; k = −16.6 ± 4.5; −16.4 ± 6.1, for FLNa KO and FLNA WT cells, respectively).

(D) Mean (±SEM) SAC activity (NPo at −70 mmHg) of FLNa KO (white) and FLNa WT (black) cells transfected with mock (GFP) or TRPP2. ** represents significant differences between TRPP2- and mock-transfected condition ($p < 0.01$); NS, not significant.

neurons where the constitutive activation of $G_{i/o}$ proteins by TRPP1 can be reversed by TRPP2 (Delmas et al., 2002). Therefore, independent function and antagonism between TRPP1 and TRPP2 are not unique to SAC regulation.

The inhibition of SAC mechanosensitivity by TRPP2 may be the result of several direct or indirect actions. One possible mechanism is that free TRPP2 interacts directly with endogenous SACs, thus acting as a dominant-negative subunit. Indeed, several TRP subunits, some of which were proposed to be involved in mechanotransduction, including TRPC1 and TRPV4, interact with TRPP2 (Kottgen et al., 2008; Tsiokas et al., 1999). However, none of those subunits had any effect on SAC activity in the present study.

Alternatively, TRPP2 may affect SAC activity by interacting with regulatory proteins, including elements of the cytoskeleton such as α-actinin, CD2AP, mDia1, tropomyosin-1, and troponin I (for reviews see Chen et al., 2008; Delmas, 2004; Harris and Torres, 2009; Wilson, 2004). Here, we show that the actin cytoskeleton is indeed implicated in SAC inhibition by TRPP2, as this effect was abolished by F-actin disruption. Moreover, the actin stabilizer jasplakinolide mimicked the effect of TRPP2 and inhibited SAC activity, as expected from a stiffening of the cytoskeleton (mechanoprotection). Additionally, we show that FLNa is a novel cytoskeletal element interacting with TRPP2. FLNa stiffens the cell cortex by virtue of its ability to crosslink adjacent actin filaments and increases actin polymerization/gelation rates in vitro (for review see Stossel et al., 2001). Consequently, localized increases in FLNa may cause an accumulation of crosslinked F-actin in the cell cortex and reduce SAC activity (D'Addario et al., 2001; Kainulainen et al., 2002). Here, we demonstrate that the activity of nonselective SACs is reduced in the presence of FLNa and that the inhibitory effect of TRPP2 is abolished when FLNa is absent. However, we cannot exclude the possibility that TRPP2 could directly interact with the SAC subunits, acting as negative regulator, but in a FLNa/F-actin-dependent manner. According to this scheme, TRPP2 could also be considered as a SACs-FLNa linker.

Because the inhibitory effect of TRPP2 was present in the mutant TRPP2-742X, which lacks an ER retention signal and is thus more efficiently targeted to the plasma membrane, as well as in the WT TRPP2, which is mainly found in the ER (Chen et al., 2001; Mochizuki et al., 1996), the subcellular localization of TRPP2 (ER versus plasma membrane) does not appear to be essential for SAC inhibition (Figure S6).

Previous work on cloned SACs, including the bacterial channel MscL or the mammalian channel TREK-1, indicate that these channels are directly activated by membrane tension (the bilayer model) (Honoré et al., 2006; Kung, 2005; Sukharev et al., 1994). The cortical cytoskeleton divides the bilayer into submicrometer microdomains (Hamill and McBride, 1997; Sachs and Morris, 1998) whose radius of curvature is much smaller than the radii of the patch or the cell (Figure 7). According to Laplace's law, T = Pr/2 (where T is tension, P pressure, and r radius of patch curvature), tension in the bilayer decreases with the radius of curvature (Hamill and McBride, 1997; Sachs and Morris, 1998). Disruption of the cytoskeleton either chemically (latrunculin A)

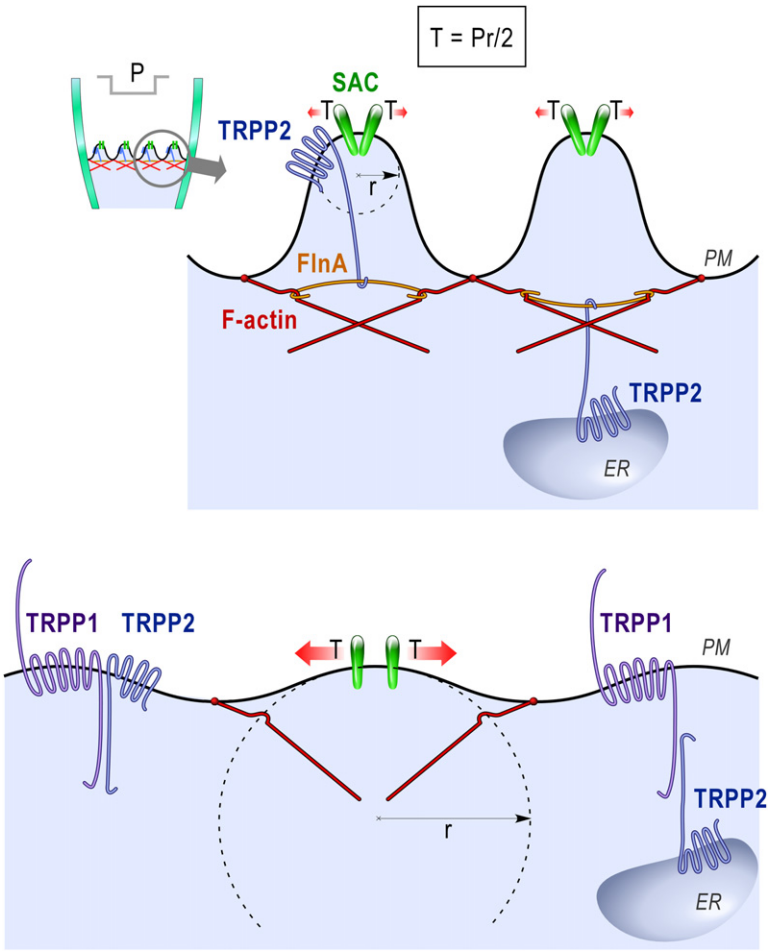

Figure 7. Cartoon Illustrating the Bilayer Convoluted by the Anchoring Cytoskeleton—"The Upholstery Model"

With a given pressure (P) drop across the patch, the tension (T) in the microdomain bilayer (~100 nm scale) is a function of their radius (r) of curvature rather than that of the mean curvature of the patch. TRPP2 is represented at the plasma membrane and in the membrane of the ER. The cytoskeleton lattice mechanically reinforces the bilayer-protecting channels from excess force. TRPP2 binding to FLNa increases actin cross-linking and makes the microdomains smaller, so that according to of Laplace's Law (T = Pr/2) there will be less tension for a given pressure. When TRPP2 or FLNa is absent, when TRPP1 is coexpressed with TRPP2, or when the actin cytoskeleton is disrupted with latrunculin A or cytochalasin D, the microdomain radius of curvature increases, resulting in a stronger activation of SACs for a given pressure.

or mechanically results in an increase in the radius of curvature of microdomains, leading to an increase in tension and SAC activity for a given transmembrane pressure (Hamill and McBride, 1997; Sachs and Morris, 1998; Wan et al., 1999). This mechanism explains the increase in channel mechanosensitivity after cytoskeleton disruption (Hamill and McBride, 1997; Wan et al., 1999). The data show that TRPP2 has the opposite effect, inhibiting SAC function via FLNa that reinforces F-actin (Figure 7).

This study is the first direct demonstration for the role of polycystins in pressure sensing. The TRPP1/TRPP2 ratio controls SAC mechanosensitivity through FLNa coupled to the actin cytoskeleton and affects the conversion of intraluminal pressure to local bilayer tension. Our findings reveal a novel molecular mechanism explaining how polycystins regulate cellular mechanosensitivity. This study is not only relevant to ADPKD but may also be of importance for a better understanding of other physiological or disease states associated with pressure sensing.

EXPERIMENTAL PROCEDURES

Dissociation of Vascular Smooth Muscle Cells

Male 12–16 weeks old mice of all three genotypes (*Pkd1*$^{+/+}$, *Pkd1SM*$^{del/+}$, and *Pkd1SM*$^{del/del}$) were used. Mice were anesthetized using isoflurane and their gut was excised. A third-order mesenteric artery (<200 μm internal diameter, 3 to 5 mm length) was dissected and incubated (20 min at 37°C) in a solution of papain (1 mg/ml) and DTT (1 mg/ml), followed by a second incubation (5 min at 37°C) in a solution of collagenase F (0.7 mg/ml) and collagenase H (0.3 mg/ml). The papain/DTT and collagenase mixture was dissolved in DCML solution, composed of 140 mM NaCl , 5.6 mM KCl, 2 mM $MgCl_2$, 10 mM HEPES, 10 mM glucose, 0.1 mM $CaCl_2$, and 1 mg/ml bovine serum albumin. Arteries were rinsed three times in DCML solution and triturated. Cell suspensions were placed on 35 mm poly-D-lysine-coated dishes and kept at 4°C for at least 45 min before recording. Recordings were only performed on elongated cells.

Electrophysiology

Electrophysiological procedure has been previously described elsewhere (Chemin et al., 2005). Single channel cell-attached recordings were performed on acutely dissociated VSMCs at a holding potential (V_{hold}) of −80 mV. Unless stated otherwise, pipette solution contained 140 mM NaCl, 5 mM KCl, 1 mM $CaCl_2$, 1 mM $MgCl_2$, 10 mM TEA-Cl, 5 mM 4-AP, and 10 mM HEPES (pH 7.35). Bath solution contained 140 mM KCl, 1 mM $MgCl_2$, 10 mM HEPES, and 10 mM glucose (pH 7.25). The osmolality of all solutions was adjusted to about 320 mOsm. Membrane patches were stimulated with brief negative pressure pulses, from 0 to −100 mm Hg in steps of −10 mm Hg, through the recording electrode using a pressure-clamp device (ALA High Speed Pressure Clamp-1 system; ALA-scientific). In whole-cell recordings, for recording L-type Ca^{2+} channel currents, pipette solution contained 110 mM CsCl, 20 mM TEA-Cl, 3 mM Na_2ATP, 3.5 mM $MgCl_2$, 10 mM EGTA, 10 mM HEPES (pH 7.25) (300 mOsm). Bath solution contained 135 mM NaCl, 5 mM KCl, 10 mM $BaCl_2$, 1 mM $MgCl_2$, 10 mM HEPES, 10 mM glucose, 0.1 μM tetrodotoxin (pH 7.35). Cell capacitance was noted for each recording, and no difference was observed between *Pkd1*$^{+/+}$ (28.0 ± 1.7 pF; n = 22) and *Pkd1SM*$^{del/del}$ (25.5 ± 1.6 pF; n = 15; p = 0.23) cells. VSMCs were stimulated from a holding voltage of −60 mV with brief (0.4 s) voltage steps from −90 to +60 mV in 10 mV increments. After a protocol with normal external solution, a second one was performed in the presence of 2 μM nifedipine. Subtracted current traces (control – nifedipine) are shown in Figure 2.

For experiments with cultured cells, the pipette medium contained 150 mM NaCl, 5 mM KCl, 1 mM $CaCl_2$, and 10 mM HEPES (pH 7.4 with NaOH). The bath medium contained 155 mM KCl, 5 mM EGTA, 3 mM $MgCl_2$, and 10 mM HEPES 10 (pH 7.2 with KOH). The osmolality of all solutions was adjusted to about 320 mOsm. For ion-selectivity experiments, the external NaCl was replaced by either sodium gluconate or choline chloride. In whole-cell recordings, F11 cells were superfused with normal bath NaCl solution, with bath solution at pH 5.5 (for the ASIC channels), or with bath solution containing a cocktail of K^+ channel blockers (10 mM TEA, 5 mM 4-AP, and 10 μM glibenclamide). V_{hold}

for all experiments was −80 mV. For K^+ channel activity the cells were stimulated with a voltage ramp (−100 to +100 mV; 1 s). Current density was determined by dividing the subtracted current [stimulated current (pH 5.5) – baseline current (pH 7.4)] by the cell capacitance, for the ASIC currents. Current density was determined by dividing the subtracted current [current at +80 mV (no blockers) – current at +80 mV (in the presence of K^+ channel blockers)] by the cell capacitance, for the K^+ currents.

Cytoskeleton-disrupting agents (Sigma-Aldrich) were used as described in the figure legends. Actin and tubulin polymerization was visualized by immunofluorescence microscopy.

Isobaric Arteriography

Male mice aged between 12 and 16 weeks of all genotypes were used. Mice were anesthetized using isoflurane and their was gut excised. A third-order mesenteric artery (<200 μm internal diameter, 3 to 5 mm long) was dissected, cannulated at both ends, and mounted in a video-monitored perfusion system as previously described (Halpern and Kelley, 1991). The arterial segment was bathed in a physiological solution (PSS) composed of 119 mM NaCl 119, 4.7 mM KCl, 2.5 mM $CaCl_2$, 1.17 mM $MgSO_4$, 25 mM $NaHCO_3$, 1.18 mM KH_2PO_4, 0.027 mM EDTA, and 5.5 mM glucose, oxygenated with a mixture of CO_2 (5%) and O_2 (20%) in N_2. The artery was pressurized at 75 mm Hg and its diameter and wall thickness were measured and recorded continuously using a video monitoring system (Living System Instrumentation Inc.). Data were collected using the Spike2 software (CED) and analyzed offline. Vessels were first allowed to stabilize for at least 30 min and were then stimulated with 80 mM KCl to verify vessel viability. Next, endothelium integrity was assessed by testing the vasodilator effect of acetylcholine (1 μM) after preconstriction with phenylephrine (1 μM). Then, a pressure diameter curve (active curve) was established by increasing intraluminal pressure from 10 to 125 mm Hg in a stepwise fashion (10, 25, 50, 75, 100, and 125). Pressure was then brought back to 75 mm Hg and the PSS solution was changed to one without $CaCl_2$ and with EGTA (5 mM), sodium nitroprusside (50 μM), and papaverine (50 μM). After a 15 min incubation in the Ca-free PSS, a pressure-diameter curve (passive curve) was performed. The KCl and phenylephrine responses were calculated using the following formula: $(D - D_{75P})/D_{75P}$; where D is the amplitude of contraction and D_{75P} is the lumen diameter under passive conditions at 75 mm Hg. Percentage of myogenic tone at each pressure was calculated using the following formula: $[(D_{pass} - D_{act})/D_{pass}] \times 100$, where D_{pass} is the diameter under passive conditions and D_{act} under active conditions. Stress-strain curves, an index of arterial elasticity, were established using the following formulas. Stress: $[(0.00133 \times P_x \times D_{Px})/(W_L + W_R)]$; where P_x is the pressure (mm Hg), D_{Px} the passive diameter at pressure x, and W_L and W_R are the thickness of the left and right walls, respectively (in μm). Strain: $[(D_{Px} - D_{P10})/D_{P10}]$, where D_{P10} is the diameter at 10 mm Hg.

Cell culture, transfection, generation, and breeding of smooth muscle-specific *Pkd1* knockout mice, arterial pressure measurements, molecular biology, siRNA transfection, real-time quantitative PCR, protein analysis, immunohistochemistry, proteomic screen, and immunoprecipitation methods are described in Supplemental Experimental Procedures.

SUPPLEMENTAL DATA

Supplemental Data contain Supplemental Experimental Procedures, 12 figures, and one table and can be found with this article online at http://www.cell.com/supplemental/S0092-8674(09)01125-8.

ACKNOWLEDGMENTS

We are grateful to the ANR 2005 cardiovasculaire-obésité-diabète, to the ANR 2008 du gène à la physiopathologie, to the Association for information and research on genetic kidney disease France, to the Fondation del Duca, to the Fondation de la recherche médicale, to the Fondation de France, to EEC Marie-Curie fellowship 039328 (J.H.A.F.), to the Fondation de recherche sur l'hypertension artérielle, to the Fondation de la recherche sur le cerveau, to the Human Frontier Science Program long-term fellowship LT-00555 (R.S.N.), to the Société Générale AM, to the Université de Nice Sophia Antipolis, and to the Centre National de la Recherche Scientifique for financial support. We are grateful to T.P. Stossel for providing the M2 and A7 cell lines and FLNa constructs and to L. Tsokias for providing the human and mouse *Pkd2* clones. We are grateful to G. Romey and J. Barhanin for valuable discussions.

Received: May 14, 2009
Revised: July 13, 2009
Accepted: August 31, 2009
Published: October 29, 2009

REFERENCES

Aboualaiwi, W.A., Takahashi, M., Mell, B.R., Jones, T.J., Ratnam, S., Kolb, R.J., and Nauli, S.M. (2009). Ciliary polycystin-2 is a mechanosensitive calcium channel involved in nitric oxide signaling cascades. Circ. Res. *104*, 860–869.

Arnaout, M.A. (2001). Molecular genetics and pathogenesis of autosomal dominant polycystic kidney disease. Annu. Rev. Med. *52*, 93–123.

Boulter, C., Mulroy, S., Webb, S., Fleming, S., Brindle, K., and Sandford, R. (2001). Cardiovascular, skeletal, and renal defects in mice with a targeted disruption of the Pkd1 gene. Proc. Natl. Acad. Sci. USA *98*, 12174–12179.

Brayden, J.E., Earley, S., Nelson, M.T., and Reading, S. (2008). Transient receptor potential (TRP) channels, vascular tone and autoregulation of cerebral blood flow. Clin. Exp. Pharmacol. Physiol. *35*, 1116–1120.

Chemin, J., Patel, A.J., Duprat, F., Lauritzen, I., Lazdunski, M., and Honoré, E. (2005). A phospholipid sensor controls mechanogating of the K^+ channel TREK-1. EMBO J. *24*, 44–53.

Chen, X.Z., Segal, Y., Basora, N., Guo, L., Peng, J.B., Babakhanlou, H., Vassilev, P.M., Brown, E.M., Hediger, M.A., and Zhou, J. (2001). Transport function of the naturally occurring pathogenic polycystin-2 mutant, R742X. Biochem. Biophys. Res. Commun. *282*, 1251–1256.

Chen, X.Z., Li, Q., Wu, Y., Liang, G., Lara, C.J., and Cantiello, H.F. (2008). Submembraneous microtubule cytoskeleton: interaction of TRPP2 with the cell cytoskeleton. FEBS J. *275*, 4675–4683.

Christensen, A.P., and Corey, D.P. (2007). TRP channels in mechanosensation: direct or indirect activation? Nat. Rev. Neurosci. *8*, 510–521.

Cunningham, C.C., Gorlin, J.B., Kwiatkowski, D.J., Hartwig, J.H., Janmey, P.A., Byers, H.R., and Stossel, T.P. (1992). Actin-binding protein requirement for cortical stability and efficient locomotion. Science *255*, 325–327.

D'Addario, M., Arora, P.D., Fan, J., Ganss, B., Ellen, R.P., and McCulloch, C.A. (2001). Cytoprotection against mechanical forces delivered through beta 1 integrins requires induction of filamin A. J. Biol. Chem. *276*, 31969–31977.

Delmas, P. (2004). Polycystins: from mechanosensation to gene regulation. Cell *118*, 145–148.

Delmas, P., Nomura, H., Li, X., Lakkis, M., Luo, Y., Segal, Y., Fernandez-Fernandez, J.M., Harris, P., Frischauf, A.M., Brown, D.A., and Zhou, J. (2002). Constitutive activation of G-proteins by polycystin-1 is antagonized by polycystin-2. J. Biol. Chem. *277*, 11276–11283.

Giamarchi, A., Padilla, F., Coste, B., Raoux, M., Crest, M., Honoré, E., and Delmas, P. (2006). The versatile nature of the calcium-permeable cation channel TRPP2. EMBO Rep. *7*, 787–793.

Glogauer, M., Arora, P., Chou, D., Janmey, P.A., Downey, G.P., and McCulloch, C.A. (1998). The role of actin-binding protein 280 in integrin-dependent mechanoprotection. J. Biol. Chem. *273*, 1689–1698.

Gottlieb, P., Folgering, J., Maroto, R., Raso, A., Wood, T.G., Kurosky, A., Bowman, C., Bichet, D., Patel, A., Sachs, F., et al. (2007). Revisiting TRPC1 and TRPC6 mechanosensitivity. Pflugers Arch. *455*, 1097–1103.

Halpern, W., and Kelley, M. (1991). In vitro methodology for resistance arteries. Blood Vessels *28*, 245–251.

Hamill, O.P., and McBride, D., Jr. (1997). Induced membrane hypo/hyper-mechanosensitivity: a limitation of patch- clamp recording. Annu. Rev. Physiol. *59*, 621–631.

Hanaoka, K., Qian, F., Boletta, A., Bhunia, A.K., Piontek, K., Tsiokas, L., Sukhatme, V.P., Guggino, W.B., and Germino, G.G. (2000). Co-assembly of polycystin-1 and −2 produces unique cation-permeable currents. Nature *408*, 990–994.

Harris, P.C., and Torres, V.E. (2009). Polycystic kidney disease. Annu. Rev. Med. *60*, 321–337.

Hill, M.A., Davis, M.J., Meininger, G.A., Potocnik, S.J., and Murphy, T.V. (2006). Arteriolar myogenic signalling mechanisms: implications for local vascular function. Clin. Hemorheol. Microcirc. *34*, 67–79.

Holtwick, R., Gotthardt, M., Skryabin, B., Steinmetz, M., Potthast, R., Zetsche, B., Hammer, R.E., Herz, J., and Kuhn, M. (2002). Smooth muscle-selective deletion of guanylyl cyclase-A prevents the acute but not chronic effects of ANP on blood pressure. Proc. Natl. Acad. Sci. USA *99*, 7142–7147.

Honoré, E., Patel, A.J., Chemin, J., Suchyna, T., and Sachs, F. (2006). Desensitization of mechano-gated *K2P* channels. Proc. Natl. Acad. Sci. USA *103*, 6859–6864.

Kainulainen, T., Pender, A., D'Addario, M., Feng, Y., Lekic, P., and McCulloch, C.A. (2002). Cell death and mechanoprotection by filamin a in connective tissues after challenge by applied tensile forces. J. Biol. Chem. *277*, 21998–22009.

Kottgen, M., Buchholz, B., Garcia-Gonzalez, M.A., Kotsis, F., Fu, X., Doerken, M., Boehlke, C., Steffl, D., Tauber, R., Wegierski, T., et al. (2008). TRPP2 and TRPV4 form a polymodal sensory channel complex. J. Cell Biol. *182*, 437–447.

Kung, C. (2005). A possible unifying principle for mechanosensation. Nature *436*, 647–654.

Lauritzen, I., Chemin, J., Honoré, E., Jodar, M., Guy, N., Lazdunski, M., and Jane Patel, A. (2005). Cross-talk between the mechano-gated K2P channel TREK-1 and the actin cytoskeleton. EMBO Rep. *6*, 642–648.

Lee, H.A., Baek, E.B., Park, K.S., Jung, H.J., Kim, J.I., Kim, S.J., and Earm, Y.E. (2007). Mechanosensitive nonselective cation channel facilitation by endothelin-1 is regulated by protein kinase C in arterial myocytes. Cardiovasc. Res. *76*, 224–235.

Maroto, R., Raso, A., Wood, T.G., Kurosky, A., Martinac, B., and Hamill, O.P. (2005). TRPC1 forms the stretch-activated cation channel in vertebrate cells. Nat. Cell Biol. *7*, 179–185.

Mederos y Schnitzler, M., Storch, U., Meibers, S., Nurwakagari, P., Breit, A., Essin, K., Gollasch, M., and Gudermann, T. (2008). Gq-coupled receptors as mechanosensors mediating myogenic vasoconstriction. EMBO J. *27*, 3092–3103.

Mochizuki, T., Wu, G., Hayashi, T., Xenophontos, S.L., Veldhuisen, B., Saris, J.J., Reynolds, D.M., Cai, Y., Gabow, P.A., Pierides, A., et al. (1996). PKD2, a gene for polycystic kidney disease that encodes an integral membrane protein. Science *272*, 1339–1342.

Morel, N., Vandenberg, G., Ahrabi, A.K., Caron, N., Desjardins, F., Balligand, J.L., Horie, S., and Devuyst, O. (2009). PKD1 haploinsufficiency is associated with altered vascular reactivity and abnormal calcium signaling in the mouse aorta. Pflugers Arch. *457*, 845–856.

Morris, C.E. (2001). Mechanoprotection of the plasma membrane in neurons and other non-erythroid cells by the spectrin-based membrane skeleton. Cell. Mol. Biol. Lett. *6*, 703–720.

Nauli, S.M., and Zhou, J. (2004). Polycystins and mechanosensation in renal and nodal cilia. Bioessays *26*, 844–856.

Nauli, S.M., Alenghat, F.J., Luo, Y., Williams, E., Vassilev, P., Li, X., Elia, A.E., Lu, W., Brown, E.M., Quinn, S.J., et al. (2003). Polycystins 1 and 2 mediate mechanosensation in the primary cilium of kidney cells. Nat. Genet. *33*, 129–137.

Nauli, S.M., Kawanabe, Y., Kaminski, J.J., Pearce, W.J., Ingber, D.E., and Zhou, J. (2008). Endothelial cilia are fluid shear sensors that regulate calcium signaling and nitric oxide production through polycystin-1. Circulation *117*, 1161–1171.

Nilius, B., Owsianik, G., Voets, T., and Peters, J.A. (2007). Transient receptor potential cation channels in disease. Physiol. Rev. *87*, 165–217.

Pedersen, S.F., and Nilius, B. (2007). Transient receptor potential channels in mechanosensing and cell volume regulation. Methods Enzymol. *428*, 183–207.

Pennekamp, P., Karcher, C., Fischer, A., Schweickert, A., Skryabin, B., Horst, J., Blum, M., and Dworniczak, B. (2002). The ion channel polycystin-2 is required for left-right axis determination in mice. Curr. Biol. *12*, 938–943.

Qian, Q., Li, M., Cai, Y., Ward, C.J., Somlo, S., Harris, P.C., and Torres, V.E. (2003). Analysis of the polycystins in aortic vascular smooth muscle cells. J. Am. Soc. Nephrol. *14*, 2280–2287.

Sachs, F., and Morris, C.E. (1998). Mechanosensitive ion channels in nonspecialized cells. Rev. Physiol. Biochem. Pharmacol. *132*, 1–77.

Spassova, M.A., Hewavitharana, T., Xu, W., Soboloff, J., and Gill, D.L. (2006). A common mechanism underlies stretch activation and receptor activation of TRPC6 channels. Proc. Natl. Acad. Sci. USA *103*, 16586–16591.

Stossel, T.P., Condeelis, J., Cooley, L., Hartwig, J.H., Noegel, A., Schleicher, M., and Shapiro, S.S. (2001). Filamins as integrators of cell mechanics and signalling. Nat. Rev. Mol. Cell Biol. *2*, 138–145.

Suchyna, T.M., Johnson, J.H., Hamer, K., Leykam, J.F., Gage, D.A., Clemo, H.F., Baumgarten, C.M., and Sachs, F. (2000). Identification of a peptide toxin from Grammostola spatulata spider venom that blocks cation-selective stretch-activated channels. J. Gen. Physiol. *115*, 583–598.

Sukharev, S.I., Blount, P., Martinac, B., Blattner, F.R., and Kung, C. (1994). A large-conductance mechanosensitive channel in *E. coli* encoded by mscL alone. Nature *368*, 265–268.

Tsiokas, L., Arnould, T., Zhu, C., Kim, E., Walz, G., and Sukhatme, V.P. (1999). Specific association of the gene product of PKD2 with the TRPC1 channel. Proc. Natl. Acad. Sci. USA *96*, 3934–3939.

Voets, T., and Nilius, B. (2009). TRPCs, GPCRs and the Bayliss effect. EMBO J. *28*, 4–5.

Wan, X., Juranka, P., and Morris, C.E. (1999). Activation of mechanosensitive currents in traumatized membrane. Am. J. Physiol. *276*, C318–C327.

Wilson, P.D. (2004). Polycystic kidney disease. N. Engl. J. Med. *350*, 151–164.